REAL-TIME SURFACE DEFECT MEASUREMENT FROM ROAD PROFILE

by

VIVEK JOLLY

Presented to the Faculty of the Graduate School of
The University of Texas at Arlington in Partial Fulfillment
of the Requirements
for the Degree of

MASTER OF SCIENCE IN ELECTRICAL ENGINEERING

THE UNIVERSITY OF TEXAS AT ARLINGTON

May 2015

Acknowledgements

I would like to thank all the people who have helped and inspired me during my master's thesis and study, especially my research advisor, Dr. Roger Walker, for his guidance during my time at The University of Texas at Arlington. His constant encouragement and support made it has been a key factor in the completion of this study. He was always available and willing to help me and my colleagues with the research. As a result I was successfully able to complete my research work and write this thesis.

Dr. Jonathan Bredow, the chairman of Electrical Engineering department, and Dr. Michael T. Manry have been very supportive as my thesis committee members and have offered advice and suggestion whenever I needed them.

All my colleagues at the Transportation and Instrumentation Laboratory made it a hospitable place to work. In particular, I would like to thank Ajit Modi and Vikram Simha for their support over the past two years.

I would also like to thank my colleagues at Broadcom Corporation especially Gigi Sebastian, Rayees Shamsuddin and Srinivasu Vantipalli for their constant support and suggestions over the six months I spent there.

Last but not the least; I would like to thank my parents for their support throughout my studies and their faith which made it possible for me to reach at this level.

April 9, 2015

Abstract

REAL-TIME SURFACE DEFECT MEASUREMENT

FROM ROAD PROFILE

Vivek Jolly, MS

The University of Texas at Arlington, 2015

Supervising Professor: Roger Walker

The Texas Department of Transportation (TxDOT) annually collects profile data over the state maintained highway network and uses the profile data to determine the ride quality based on a serviceability index (SI) and the International Roughness Index (IRI). The equation used at present to obtain the SI from the profile data is based on ride measurements from an old rating session in the 1960s. Several changes have taken place over the years that required re-evaluation of the ride equation, led to a TxDOT funded research in 2000 to evaluate the adequacy of the current equation. During this study, a new ride equation or NSI was developed and found to correlate much better to how the travelling public rates pavements than the old ride equation IRI. This thesis is aimed at developing a real-time multi-threaded embedded module and program that can be used with a portable profiler for measuring NSI. It also includes investigations on the effectiveness of the new ride equation from recent profile and resulting IRI measurements. Specifically, this study investigates the use of a real-time system to calculate the NSI (New Serviceability Index), the index generated by the new ride equation.

This thesis focuses on collecting simulated profile data for a stretch of the road and calculating the roughness index for each section. The minimum size of the sections is 52.8ft or 0.01miles. Simulations are generated based on the profile data generated by the laser and accelerometer readings at the profiler. These profile simulations are processed in real-time, as soon as the data for each user-specified section length is available, using the new ride equation. This calculates the NSI for each section and the resulting NSI values are displayed. Investigations are also included comparing the NSI to IRI for profile obtained from a number of different pavement types measured during a recently completed TXDOT research project.

Table of Contents

List of Illustrations

List of Tables

Chapter 1

Introduction

The ride quality of pavements is collected periodically over the Texas highway network for different purposes including the condition of the highway network. Such measurements are reported to national agencies based on which funding is allocated to the state departments of transportation (DOT). The Texas Department of Transportation (TxDOT) is one such state department that collects this data. It is also used to ensure proper maintenance of the roadways. In order to compare the data spread over a vast area, several standard measurement techniques were devised and are still being devised by different agencies.

Based on the collected data, it is common to rate these surfaces with an index that specifies their smoothness or roughness. Several indices were developed over the years to provide an objective measure of the state of the road. The nationally accepted standard index is the International Roughness Index (IRI). Since 1990, the Federal Highway Administration (FWHA) has required states to report road roughness on the IRI scale for inclusion in the Highway Performance Monitoring System (HPMS). However, different state DOTs (Departments of Transportation) sometimes also use their own standard indices. TxDOT uses an index known as the Serviceability Index (SI), which gives a rating on a scale of 0 to 5 of the quality of the road. This index is similar to the indices used by some other states and is often related to the IRI. These indices will be discussed in detail in later Chapter 3.

1.1 Problem Definition

The above mentioned indices are typically obtained by post processing of the measured profile. Also, an index depicting the true ride quality of the road was only obtained when the primitive method of having people rate the ride quality by sitting in a

standard vehicle travelling through the specified pavement is used. However, this method had its drawbacks due to the subjective ratings as well as rater fatigues, inability to compare data, repeatability and reproducibility issues, etc. These drawbacks led to the development of the above mentioned indices. Also, for the electronic rating sessions, the distance that can be covered in a single session is small. The real-time surface defect measurement project aims to provide an embedded module that will provide NSI real-time measurements which can be stored along with the IRI. The system is able to continuously obtain and process profile data for long stretches of road irrespective of the speed of the vehicle.

Specifically, the objective of current research at the Transportation Instrumentation Lab (TIL) at the University of Texas at Arlington (UTA) is to develop a portable embedded, integrated framework that can be used for real-time measuring and monitoring of pavements.

1.2 Approach

The main components involved in the surface defect measurement system are:

- Portable Profiler
- Portable NSI processing unit supporting multithreading and real-time operation
- Real-time display unit

The research conducted and described in this thesis focuses on the processing unit which runs a multithreaded real-time application to acquire and process the data from the portable profiler.

The profiler is connected to the processing unit via a client-server LAN network, through which the road profile data is transmitted to the processing unit. Considering that the New Serviceability Index (NSI) has been experimentally proven to be a close

approximation to the ride quality ratings given by the raters, the processing unit runs the NSI ride equation on the received data and obtains the NSI value indicating the ride quality. This NSI value is displayed on the display unit for real-time viewing as well as for verification purposes.

Further chapters of the thesis include an introduction to the portable profiler, calculation of the NSI from the data obtained from this profiler, about the processing unit used and the results supporting the implementation of the surface defect measurement system.

Chapter 2

Profiler

2.1 Introduction to Profiling

2.1.1 Road Profile

Road profile is the two dimensional cross section of a road surface taken along an imaginary line. Profile gives information about roughness, design grade and texture of the road [1]. When testing a road for roughness, most of the profiling companies and state transportation departments measure the longitudinal profile of the road.

Many state transportation agencies use lasers and accelerometers to determine the profile. The car movements are filtered out from these laser and/or accelerometer readings. The Transportation Instrumentation Lab at UTA has developed a profiling algorithm that is used to compute the profile from the three sensors (2 laser sensors and 2 accelerometers). The algorithm is discussed in the later sections.

2.1.2 Pavement Profiling Methods

The high-speed pavement profilers today use one of two generally known profiling methods or their derivations. The first method, developed by Elson Spangler and William Kelly in the early 1960s, uses an accelerometer to measure the vehicle mass motion, which when double integrated gives the mass displacement, Z_m. The mass displacement with respect to the road, $(W - M)_m$, is measured by the laser beam perpendicular to the road surface. Summing the computed mass displacement, Z_m with $(W - M)_m$, or mass displacement with respect to the road, yields W_m, the measured road profile.

The second method, developed by David Huff of South Dakota Department of Transportation (SDDOT), uses a similar procedure but with a time-based algorithm. Both acceleration and the measured mass displacement with respect to road are sampled with

respect to time. The acceleration is integrated with respect to time and added to the time sampled road-body displacements. Both methods use a filtering process to attenuate the low frequencies or large wavelengths measured by the accelerometer. The portable profiler used for this project as well as other projects at the Transportation Instrumentation Laboratory uses a variation of the South Dakota method developed by Roger Walker at UTA. The Walker method combines both sampling and integration with respect to time while filtering with respect to distance.

2.2 Portable Profiler

2.2.1 Profiler Components

The portable profiler developed at the Transportation Instrumentation Lab at UTA (TX6004-2) consists of the following three sensors:

- A laser for road-body displacement measurements
- A distance encoder, to measure the distance travelled and to synchronize the computed profile to this distance
- An accelerometer to measure vehicle-body displacements.

A fourth sensor, an infrared start sensor is also used. This is used for automated and precise profile measurements for profile verification and repeatability studies.

The portable profiler developed at the Embedded Transportation Instrumentation Lab at UTA uses an LMI SLS 5000 laser (Figure 2-1) for measuring road-body displacements. The vehicle body acceleration is measured using a ± 4g Columbia Research SA107BHP accelerometer. An Accu-Coder 260 encoder is used to synchronize the computed profiles to the distance travelled.

Figure 2-1 LMI's Selcom Road Lasers

2.2.2 Instrument Module

The portable instrument module consists of sensors, power, filter and other components and these are listed in Table 2.1. Figure 2-2 shows a block diagram of the connections for these components. The distance encoder is attached to the vehicle wheel while the rest of the components including the sensors, power and signal conditioning are housed inside the profiler instrument module that is placed on the front or rear bumper of the profiler vehicle. The data collected from the sensors are digitized and sent via USB cable to a notebook PC located in the vehicle to compute the profile. A PCB contains the filter and other signal processing circuits. Figures 2-3 illustrates the schematics of these circuits and figure 2-4 shows the layout of the sensor components in the instrument module. The instrument module has four connectors as shown in figure 2-5 for power,

USB for PC, distance encoder and infrared signal. The profiler unit runs on the vehicle's 12V power source.

Table 2-1 Instrument Module Components

Item No.	Component
1	USB Connector Mount – DT 9816 to PC
2	Filter Module – SIM Board
3	DT 9816 Data Translation A/D Module
4	DC-DC Converter – 12v to 24v
5	DC-DC Converter – 12v to 5v, ±15v
6	SLS 5000 Laser
7	4g Accelerometer
8	Laser Connector Breakout
9	Power
10	R1 – 500 ohms

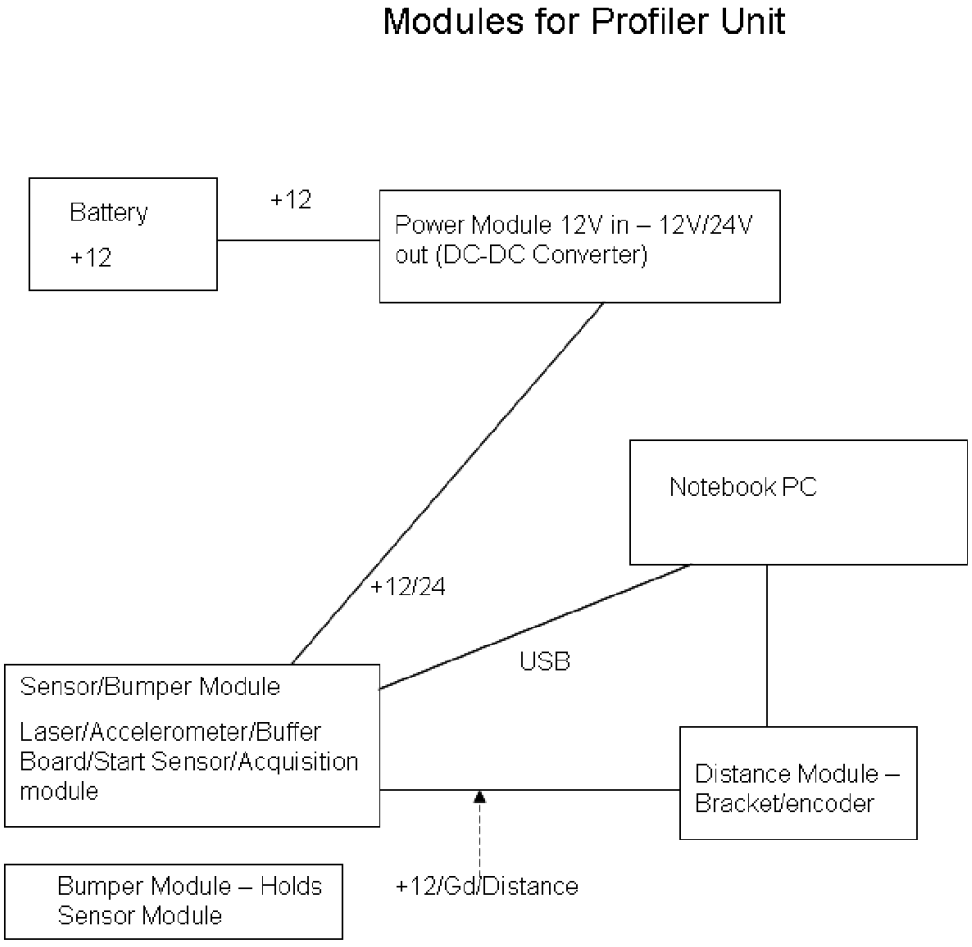

Figure 2-2 Profiler Module Block Diagram (TX6004-2)

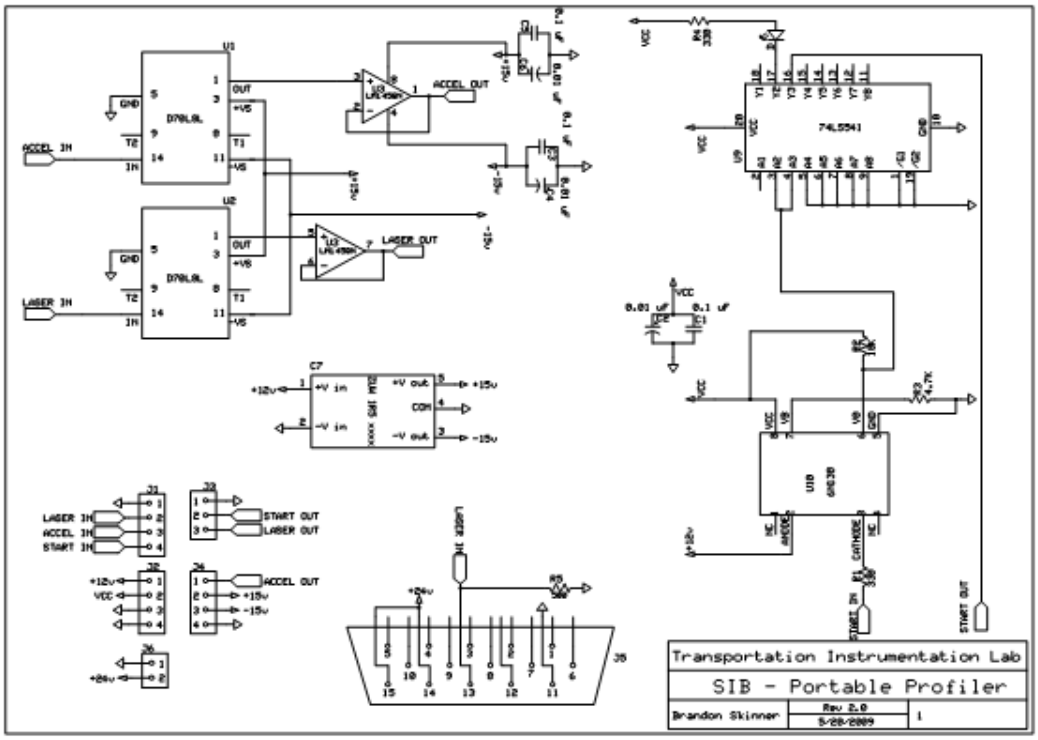

Figure 2-3 Signal Conditioning Schematic

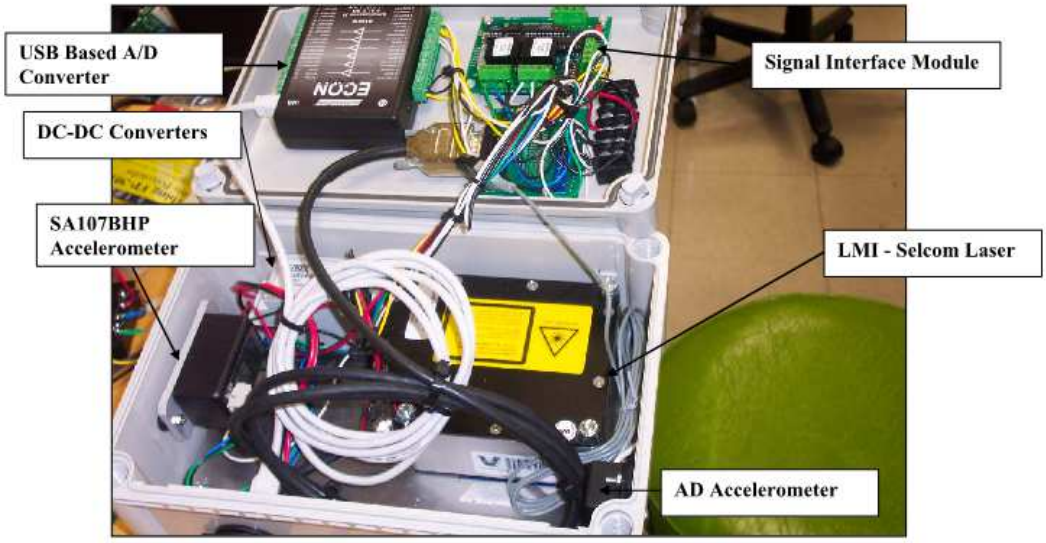

Figure 2-4 Profiler Instrument Package (TX6004-2)

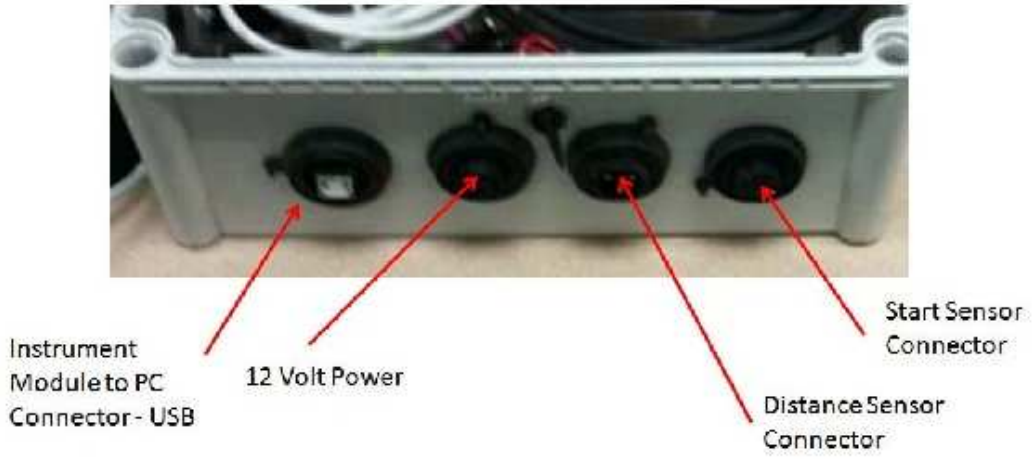

Figure 2-5 Profiler Instrument Module Connectors (TX6004-2)

2.2.3 Profiling Software

The profiler runs on a modified version of the UTA Ride Console program which was developed at The University of Texas at Arlington and has been used in TxDOT and TTI profilers for data collection and certification purposes over the years. The profiler unit provides output data confirming to the TxDOT VNET protocol.

2.2.4 Profiling Method

As mentioned earlier, the profiling method used is similar to the South Dakota method as it implements a time-based profiling algorithm. The body acceleration and road-body displacement are sampled with respect to time. The body acceleration is then integrated with respect to time and added to the time-sampled road-body displacements. A filtering process attenuates the low frequencies or large wavelengths, measured by the accelerometer. The UTA method implements a four pole IIR Butterworth cascaded filter, where the first two poles are combined with a recursive time integration process. The coefficients for the Butterworth filter are computed for each time and distance displacements using the bilinear transform. The output is then fed into the second

cascaded part of the two-pole filter. The laser displacement readings are added to the double integrated accelerometer readings during the filtering process resulting in the profile, W. Figure 2.6 illustrates the above process.

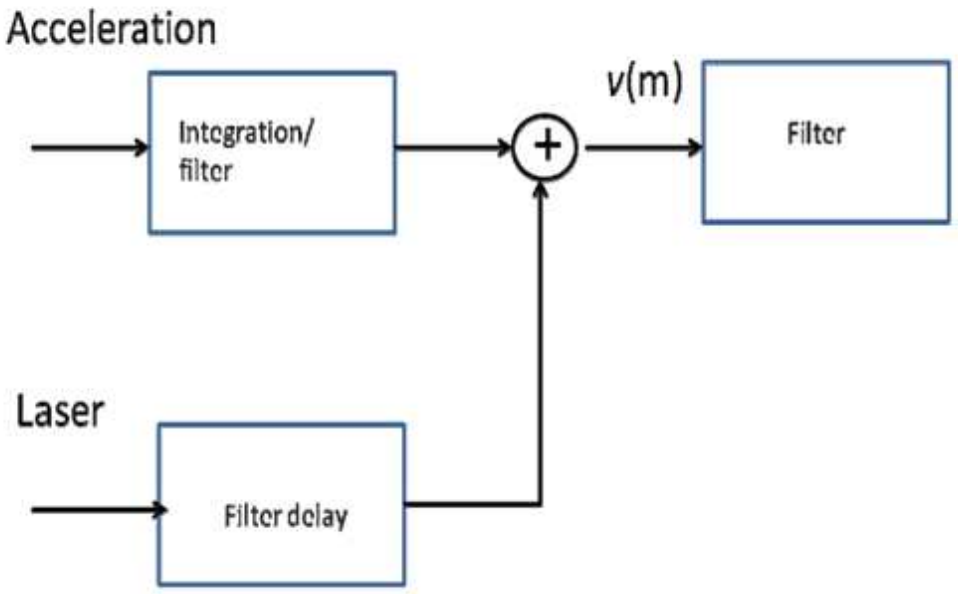

Figure 2-6 UTA Profile Computation Process (TX6004-2)

As a signal is filtered, both the amplitudes as well as the phase of the frequencies in the stop and transition bands are affected by the filter. If the filter is a linear phase filter, the phase response of the signals is a linear function of frequency. For nonlinear phase filters the fact that the response is not a linear function of the frequency can result in some undesirable characteristics. The UTA profiling procedure uses a Butterworth Infinite Impulse Response (IIR) filter, resulting in a nonlinear phase change during the filtering processing. The nonlinear phase effect results in a distance delay of the frequencies in the profile signal in the stop and transition bands, as well as many of the frequencies in the pass band. A simple illustration of the results of such a nonlinear

delay on the frequencies comprising a profile signal, is that the location of some objects, such as bumps or hills, are oriented differently from one another than from their original position. Accounting for such movements in linear phase filters is easily adjusted for as the frequencies comprising a profile signal are simply delayed but maintain their same orientation with respect to each other as in the original unfiltered signal. The effects of the nonlinear phase can also be adjusted by applying the same nonlinear filter used on the original in the reverse direction. Thus a reverse filter is applied to the profile data for project level applications.

2.2.5 UTA Profiler Program

The UTA Profiler Program, which runs in real-time, interfaces with the Data Translation DT9816 in the instrument module via USB. It averages the time-digitized sensor readings over each distance interval and computes the profile in accordance to the method described in the previous section. Figures 2-7 and 2-8 illustrate the program flow. Figure 2-9 is a sample output of the portable profiler. The data, obtained by computing the profile values, is stored in a disk in accordance to the TxDOT VNET protocol. The profile may then be used for post processing.

This project uses the profile as it is generated in real-time to calculate the New Serviceability Index (NSI) in real-time. The NSI is described in detail in the next chapter. Due to unavailability of profiler module, this project uses a simulation of the profiler that sends out profile data as the actual profiler module would send out. This data is used in real-time to calculate the NSI and thereby determine the ride quality of the road.

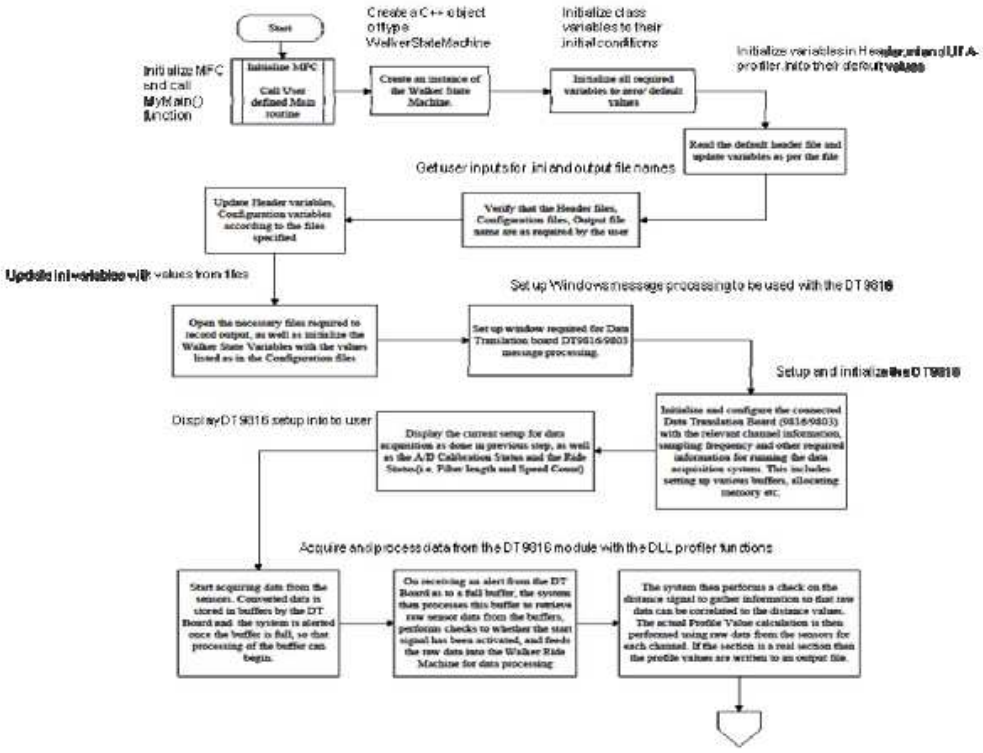

Figure 2-7 Part A of UTA Profiler Program Flow Diagram (TX6004-2)

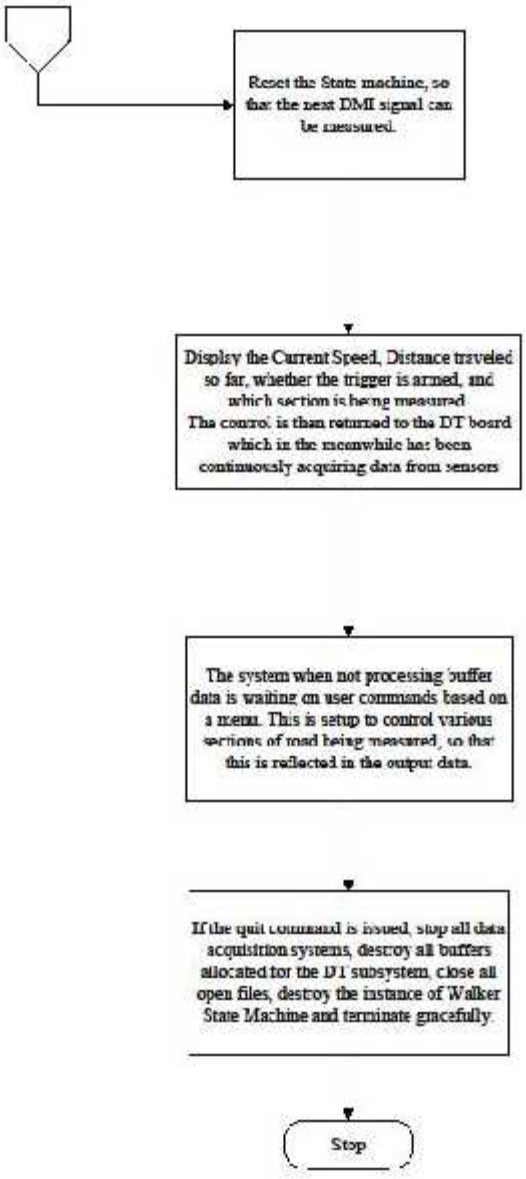

Figure 2-8 Part B of UTA Profiler Program Flow Diagram (TX6004-2)

```
HEAD3,08082012,13,076,FM1383S,478.000000 +00.100,K1
CMET3,TTIProfiler,,,,,1FTSW21P76EB82581,07062011
KPRF01,mil,LR,0.960503,i
Inverted prime (RC250 and Grade 5 aggregate)
Comment Card
157,157,0
158,158,0
158,158,0
158,158,0
158,158,0
158,158,0
158,158,0
158,158,0
158,158,0
157,157,0
156,156,0
154,154,0
153,153,0
152,152,0
151,151,0
150,150,0
149,149,0
149,149,0
150,150,0
151,151,0
151,151,0
151,151,0
150,150,0
149,149,0
149,149,0
148,148,0
146,146,0
145,145,0
144,144,0
```

Figure 2-9 Sample Output from the Portable Profiler

Chapter 3

NSI

3.1 Serviceability Index

3.1.1 Introduction to Serviceability Index

The pavement condition is typically assigned a score that is an indicator of their overall condition of the road, based on measurements of roughness and surface distress. This score quantifies a pavement's overall performance and is useful help in managing pavement networks. This index may represent either a single distress such as a crack due to fatigue or a combination of such distresses in which case it is usually referred to as a composite index. These pavement scores are useful for the following applications.

- Stimulate repairs: Once a pavement's condition reaches an unacceptable score, it can be scheduled for maintenance or rehabilitation.
- Estimate extent of damage and cost of repair: The pavement condition score is a numerical representation of the overall condition of that pavement and can therefore be used to estimate the repair work required and also the cost for these repairs.
- Determine condition index for the whole pavement network: By combining the pavement condition scores for different sections in the network, a consolidated score for the entire pavement network can be determined.
- Allow equal comparison of different pavements: The pavement condition score is based on the pavement properties measured. This gives a level ground for comparison between multiple pavements.

A pavement condition index is the scale, or a series of numbers, that represents a pavement condition. These indices may be on a scale of 0 to 5 or 0 to 100. One of the oldest indices used to depict the pavement condition is the Present Serviceability Rating (PSR), which was developed at the AASHO Road Test. An index that is currently most popular and has been adopted by many states in the development of their pavement management system (PMS) is

the Present Serviceability Index (PSI), which is a statistical approximation of the PSR. PSR is used by the Federal Highway Administration (FHWA) for nationwide road health monitoring. The PSR values range from 0 to 5. Table 3.1 provides the FWHA guidelines for collecting PSR data.

Table 3-1 FHWA guidelines for PSR data collection [2]

Verbal	Description	PSR
Very Good	Only new, superior (or nearly new) pavements are likely to be smooth enough and distress free (sufficiently free of cracks and patches) to qualify for this category. Most pavements constructed or resurfaced during the data year would normally be rated as very good.	5.0 – 4.0
Good	Pavements in this category, although not quite as smooth as those described above, give a first class ride and exhibit few, if any, visible signs of surface deterioration. Flexible pavements may be beginning to show evidence of rutting and fine random cracks. Rigid pavements may be beginning to show evidence of slight surface deterioration, such as minor cracks and spalding.	3.9 – 3.0
Fair	The riding qualities of pavements in this category are noticeably inferior to those of new pavements, and may be barely tolerable for high speed traffic. Surface defects of flexible pavements may include rutting, map cracking and extensive patching. Rigid pavements in this group may have a few joint failures, faulting and cracking, and some pumping.	2.9 – 2.0
Poor	Pavements in this category have deteriorated to such an extent that they affect the speed of free-flow traffic. Flexible pavement may have large potholes and deep cracks. Distress includes raveling, cracking, rutting, and occurs over 50 percent, or more, of the surface. Rigid pavement distress includes joint spalling, faulting, patching, cracking, scaling, and may include pumping and faulting.	1.9 – 1.0
Very Poor	Pavements in this category are in an extremely deteriorate condition. The facility is passable only at reduced speeds, and with considerable ride discomfort. Large potholes and deep cracks exist. Distress occurs over 75 percent or more of the surface.	0.9 – 0.0

3.1.2 International Roughness Index

The highway engineering community had, in the early 1980s, identified road roughness the primary method to gauge the utility of a highway network to road users. However, the existing methods used to characterize roughness were not reproducible by different agencies as they depended on different measuring equipment and methods. Nor were they stable with time. The United States National Cooperative Highway Research Program (NCHRP) initiated a research project to help state agencies improve the use of their equipment to measure roughness. The World Bank continued this work in an effort to compare or convert the data obtained different countries that were involved in World Bank projects. Findings from these tests suggested that with a standardized procedure, most of the equipments in used could produce the roughness measures on a single scale, which was eventually named the International Roughness Index (IRI).

The IRI is a mathematical property of a two-dimensional road profile. It can be determined from profiles generated by any valid method of measurement ranging from static rod and level surveying equipment to high-speed inertial profiling systems. The quarter-car math model aims to replicate the roughness measurements methods in use by highway agencies in the 1970s and 1980s. The correlation of IRI with a typical instrumented vehicle was comparable to the correlation between the measures from any two vehicles. Thus, the IRI is considered the statistical equivalent of the methods that were in use. The IRI is reproducible, repeatable and stable with time. It is based on the concept of a 'golden car' with known suspension properties and is calculated by simulating the response of this 'golden car' to the road profile with simulated vehicle speed of 80 km/h (49.7 mi/h).

3.1.3 History of Current Ride Equation [15]

The new ride equation used by TxDOT for estimating ride or PSI from profile data as well as from the IRI is considerably different from the original ride equation, which was developed from a rating session in 1968-1969. For this session, sections were rated in three

areas of Texas by what was considered the 'typical highway user' and the 'typical vehicle'. The profile of each section and the associated statistics were computed. The first model developed by Roberts and Hudson in 1970, estimated ride primarily from the slope variance statistic of the road profile. This model, although never implemented, was a pointer to use the spectral estimates of the ride model to predict the ride quality. The relationship was noted while grouping PSR with the power spectral ratings.

For this model, the wavelength amplitudes were computed from the profile and correlated to the present serviceability rating (PSR) obtained from the raters. This original equation from Walker and Hudson (1973) is given below.

$$SI = 3.41 - 1.43X_1 - 0.306X_2 - 0.180X_4 - 0.644X_5 + 1.25C_1 - 0.458X^2_2 - 1.05X^2_4 - 0.986X^2_5 + 0.841X^2_7 + 1.76X_1X_4 - 1.35X_1X_6 - 1.06X_1X_8 - 1.84X_1X_9 + 2.16X_3X_{10} + 1.21X_2X_5 + 0.741X_4X_9 + 1.51X_5X_7 - 1.65X_5X_{10} - 2.03X_7X_8 + 1.81X_8X_{10} + 0.679T$$

where

$X_1 = \log A_{0.012} - 0.426$

$X_2 = \log A_{0.023} - 0.895$

$X_3 = \log A_{0.035} + 1.481$

$X_4 = \log A_{0.046} + 1.893$

$X_5 = \log A_{0.058} + 2.139$

$X_6 = \log A_{0.069} + 2.351$

$X_7 = \log A_{0.081} + 2.500$

$X_8 = \log A_{0.092} + 2.593$

$X_9 = \log A_{0.104} + 2.670$

$X_{10} = \log A_{0.116} + 2.744$

$C_1 = \log CP_{0.012} - 0.3389$

T = Pavement type (1 for concrete and 0 for asphalt)

A_i = average of the left and right wheel path amplitudes (inches) for frequency band i in cpf

$CP_{0.012}$ = cross amplitude for the 0.012 cpf frequency band

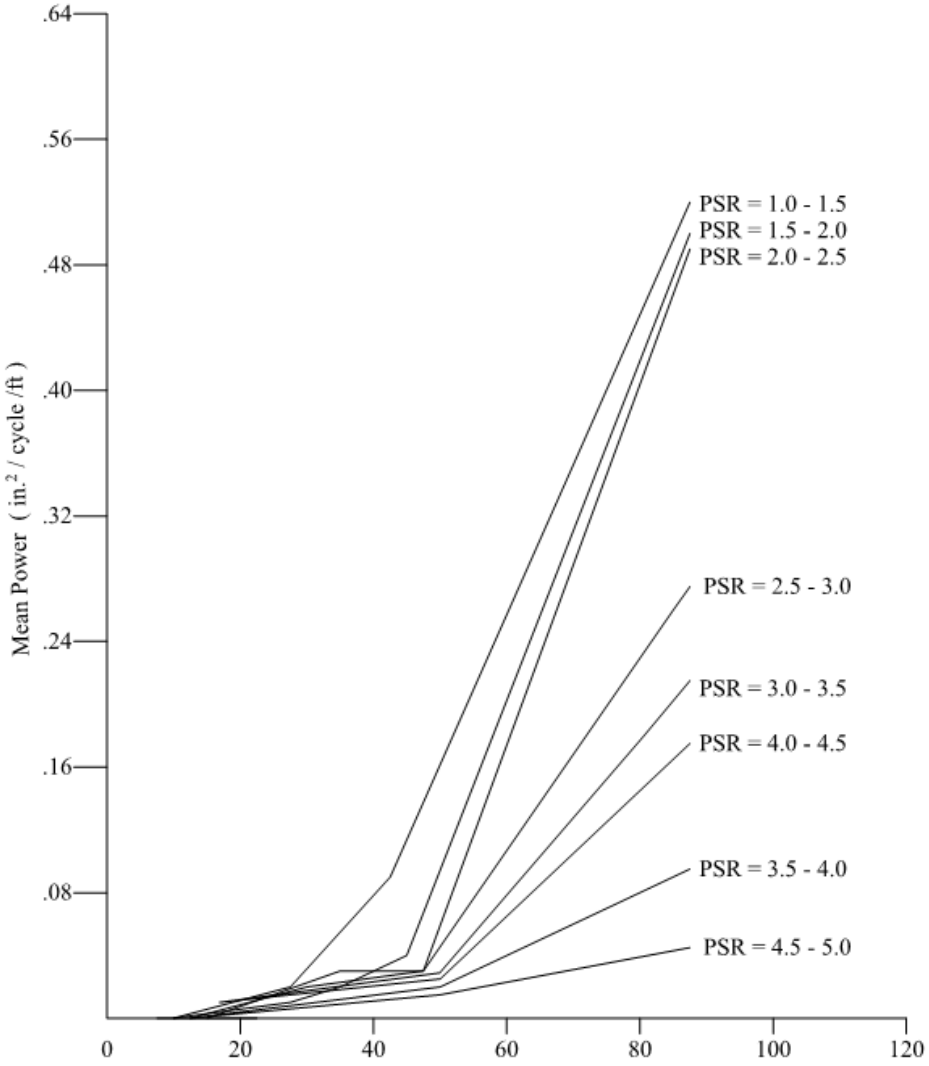

Figure 3-1 Wavelength vs. Power Spectral Data [15]

There have been several modifications to this equation over time starting from early 1980's. The earlier device used for measuring road profile (the Surface Dynamics Profilometer or SDP) was not easy to use or maintain. The Mays Ride Meter (Rainhart, 1972) was a less

sophisticated and cheaper device for measuring ride, but did not provide profile and was vehicle dependent. A procedure was developed by Walker and Hudson (1973) to use these devices in which each MRM device could be related to PSI from the MRM readings, and a lookup table was used for determining the appropriate estimated PSI readings. The SDP would be used solely for calibrating the MRM. In spite of the calibrations, the readings from the MRM were still vehicle dependent and a standard Mays Trailer was developed for each MRM that helped reduce this variation.

In 1981, a better relationship between MRM and PSI was discovered (McKenzie et al., 1982). A common relationship between the MRM devices and the road profile was determined correlated to PSI. The readings from the Mays Ride Meters in the study were correlated to the root mean square vertical acceleration (RMSVA) statistic of the road profile. The result of this established a 'standard MRM'. The 'standard MRM' was then calibrated to PSI in accordance with the procedure of McKenzie et al. (1982). These two equations for predicting PSI from the road profile are:

$$MO = -20 + 23VA_4 + 58VA_{16}$$

$$PSI = 5\exp\left([-(\ln(32\,MO))/8.4933]^{9.3566}\right)$$

With the coming of the digital era, the sensors and filtering were made digital and an emulated version of SDP was built which had a number of advantages over the first and even second generation in that lasers were used instead of the mechanical road following wheels, allowing measurement speeds to 70 miles per hour. Also, an 'off the shelf PC' was used for the digital computing requirements. This system was used until about 1995.

In 1995, TxDOT acquired a system board with a modified version of the South Dakota method for profile estimation that had been used in Europe for profile and rut measurements. With these boards, TxDOT was able to build and maintain a fleet of profiler systems (the Texas Profilers) and which are still in use today.

One of the issues with these systems is that the distance sensor used for reporting profile values is not an integer divisor of 0.5 feet or 6 inches as used by the SDP. This distance interval was one of the bases of the VERTAC model. Thus, a decision was made at that time to relate the estimated PSI from the VERTAC model to the IRI. In 1996, this model was refined to produce a better estimate of the PSI. This model also had the added advantage in that different PSI reporting intervals could be selected as all previous models were based on 0.2 miles. A 'C' function code that illustrates this model is shown below and is depicted in Figure 3-2.

```
}
float IRIToPSI(float iri) {
float psi;
#ifdef CC_ENGLISH
iri = INCH_PER_MILE_TO_MM_PER_M(iri);
#endif
psi = 8.8532704+ (-4.425873)*pow(iri,0.35);
if (psi <0)
psi = 0;
else if (psi > 4.7) {
if (psi >=5.38)
psi = 5.0;
else
psi = 4.7 + (psi-4.7) * (5.0-4.7)/(5.38-4.7);
}
return psi;
}
return psi;
```

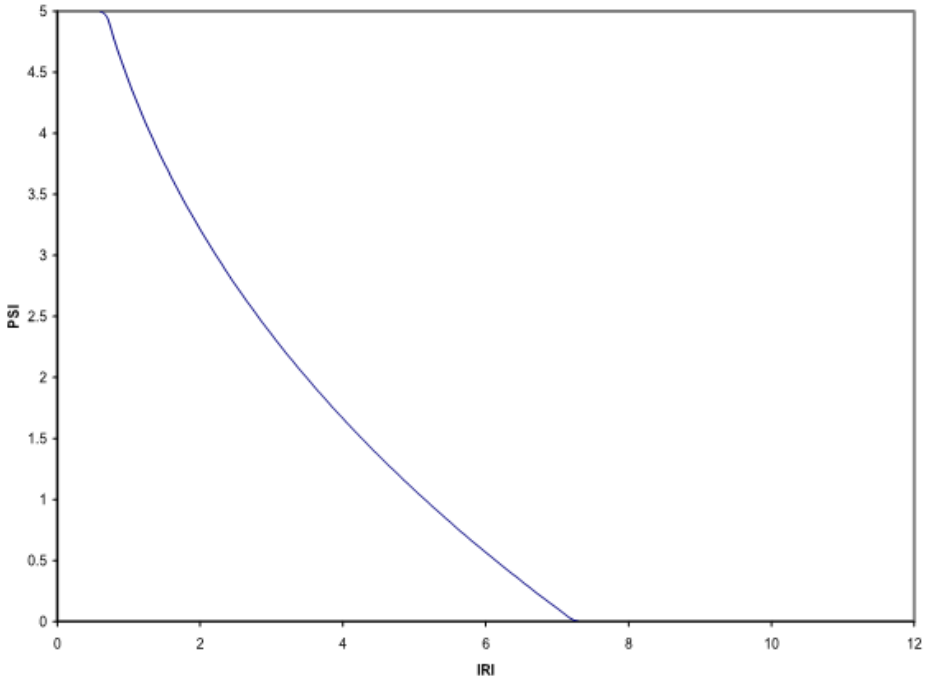

Figure 3-2 PSI vs. IRI – Current Ride Model [15]

3.2 New Ride Model

3.2.1 Model Development

The original PSI model, which is dependent on the IRI rather than the PSR, had several problems. First, when using the Fast Fourier Transform (FFT) to compute the frequency components, the center frequencies were tied directly to the number of points and the sampling interval. Since the current profiler estimates obtained from the Texas Profilers are related to the distance sensor on the profiler, this interval can vary depending on vehicle type and tire sizes. The center frequencies of the spectral estimates would hence be different for each vehicle, using a similar type model and would require interpolation or other similar adjustments when using the model. The sample interval of the original analog KJ Law Profiler and the later digital version used a fixed 0.5-foot interval. Secondly, the section length was fixed for 0.2 mile. The Pavement Management Information System (PMIS) currently uses 0.1 mile sections. Thus, it was decided that any new model should address these limitations.

The computation of the power spectral components for the 2000 rating session data was combined with the 1999 session and the results are illustrated in Figures 3-3 for 32 band computations. Since the sampling interval was different, i.e., different profilers were used for the first and second sessions, the frequency bands were made identical by increasing the data file lengths by adding zeros to the next power of two, in conjunction with interpolation of the spectral estimates to account for the differences. As more bands are used, the fundamental frequency decreases resulting in longer wavelength and fewer the degrees of freedom for each spectral estimate.

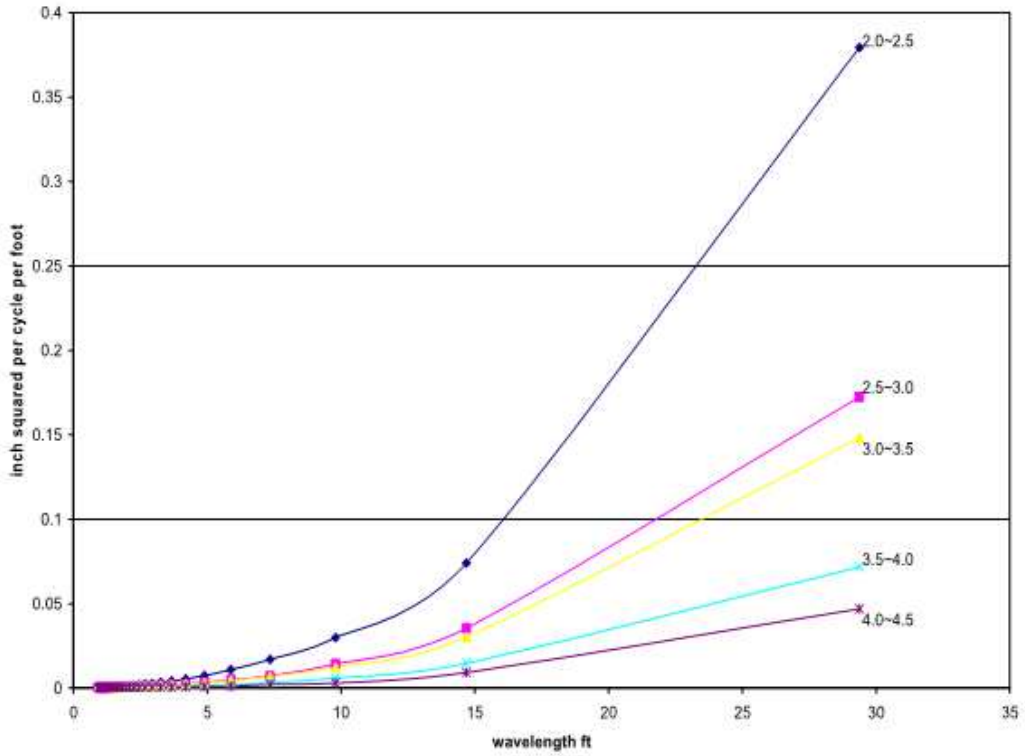

Figure 3-3 Wavelength vs. Power Spectral Rating for 32 Bands [15]

The first approach used for developing a model was to simply repeat the process used in the original model, where the independent variables would be the power at the various bands and the dependent variable, PSR. In the original model, the power estimates for each wheel path, along with the cross spectral components were considered. This led eventually to the

rather complicated model given in Chapter 3.1.2. The approach used for developing this model was to try and find a simpler, less complicated procedure. However, using the spectral estimates seemed attractive as it would be useful to relate the effects of certain frequencies on ride. A number of variations of variables and models were attempted but never resulted in satisfactory estimates any better than those found with the current IRI model.

After reviewing the correlations of the various frequency bands, it was decided to select the frequencies associated with a set of fixed, equally spaced wavelength bands, one to eight meters. This set of frequencies would cover those that are affected by the ASTM ride number, as well as the profilograph. For these frequencies, the longest wavelength is 8 meter or about 26 feet.

The independent variables, the power spectral estimate for each run, are calculated and then averaged over the same section. These estimates for each of the eight frequencies are computed directly from the Discrete Fourier Transform (DFT) in accordance with the equation 3.1:

$$X(f) = \sum_{k=0}^{N-1} x_k e^{-j2*\pi*k*f*t} \text{ , } 0 \le f \le 0.5/T \quad (3.1)$$

$$P_f = \frac{1}{N} | X_f | \quad (3.2)$$

where N = 64, f = 1/8, 2/8, … 1 cycles/meter frequencies, and X(f) is DFT and P is the spectral component associated with the frequency.

The final model selected is of the form:

$$NSI = 5e^{-\sqrt{\alpha P}} \quad (3.3)$$

where NSI or New Serviceability Index denotes the predicted PSR and αP can be described as

$$\alpha P = \alpha_1 P_1 + \alpha_2 P_2 + \ldots + \alpha_8 P_8$$

and where each P tem represents a power spectrum for each frequency component. The set of "α" coefficients are derived from the regression analysis.

Table 3-2 provides the PSR readings along with the NSI and PSI values. The standard deviation of the residuals for the new model is 0.21. The advantage of computing the direct form

of the DFT components as opposed to the FFT by this procedure is that equation 3.1 can be used to compute any set of DFT components of the profile, whether or not the frequencies are equally spaced n the frequency domain. Also, only eight spectral components need to be computed. The power of these complex frequency components are then computed by and averaged over the 0.1 mile data set.

To determine the eight frequencies, a regression analysis was performed on the eight power spectral components with PSR values as the independent variable. The regression analysis was performed with 95% confidence for the coefficients. For the regression, a subset of the combined 1999 and 2000 profile data sets were selected. The R^2 of the regression was found to be 0.87. The eight α coefficients found, beginning with the first frequency, 0.125 cycles per meter are -2.36E+06, 6.15E+06, -5.80E+06, 2.42E+06, -4.48E+05, 3.36E+04, -5.80E+06, -6.79E+01, respectively.

Table 3-2 PSR vs. NSI vs. PSI [15]

Section	PSR	New Model	Current PSI
2	3.15	3.11	3.34
3	2.92	3.05	3.14
4	3.61	3.5	3.84
5	3.53	3.12	4.2
6	3.14	3.22	3.58
7	2.68	2.89	2.38
8	2.84	3.22	3
9	2.27	2.28	1.96
10	3.18	3.25	3.2
11	3.22	3.14	2.98
12	2.34	2.66	2.18
13	2.22	2.18	1.74
14	3.58	3.27	3.28
15	3.52	3.28	3.1
16	3.34	3.27	2.84
17	2.78	2.71	2.26
18	3.55	3.52	3.34
19	2.38	2.39	2.16

Table 3-2 continued

20	3.48	3.56	3.32
21	3.44	3.45	3.5
22	3.57	3.6	3.56
23	3.5	3.47	3.58
24	3.13	3.21	3.12
25	3.04	2.98	2.97
26	3.06	2.94	3.22
27	3.31	3.08	3.2
28	2.64	2.84	3.18
29	3.52	4.02	3.72
30	3.45	3.45	3.44
31	3.9	3.84	4.3
32	3.47	3.39	3.76
33	2.47	2.27	2.06
34	2.21	2.52	2.14
39	3.73	3.67	4.1
40	3.65	3.44	4.3
41	3.77	3.68	4.14
42	3.81	3.78	4.24
44	4.05	3.98	4.36
45	3.93	3.87	4.4
46	3.9	3.86	4.3
47	3.39	3.26	3.5
48	3.69	3.82	4.2
49	3.51	3.39	3.64
50	3.85	3.58	4.12
51	3.97	3.85	4.22
52	3.9	3.96	4.52
53	3.28	3.16	3.06
54	3.64	3.33	3.56
55	3.36	3.3	3.2
56	3.79	3.32	3.56
57	3.5	3.36	3.31
58	3.03	2.95	2.98
61	4.04	3.69	4.06
62	3.32	3.12	3.16
63	3.42	3.28	3.36

Table 3-2 continued

64	3.53	3.68	3.3
65	3.59	3.55	3.44
66	3.11	3.17	2.48
67	3.39	3.28	3.6
68	3.09	3.28	3.28
69	3.53	3.93	3.54
70	3.48	3.43	3.72
71	3.53	3.87	4
72	2.57	2.51	2.82
73	3.51	3.77	4.22
74	3.38	3.23	3.5
75	2.94	2.77	2.82
76	3.59	3.28	3.84
77	3.13	3.23	3.48
78	2.55	2.65	2.74
79	3.46	3.83	4.18
80	2.68	2.62	3
81	3.52	3.15	3.12
82	1.92	1.93	1.62
83	3.91	3.82	4.4
84	3.85	3.78	4.14
85	2.87	3.15	3.55
86	2.84	3.33	3.44
90	3.57	3.55	3.77
98	2.86	2.85	2.8
99	3.52	3.78	4.23
100	3.63	3.77	4.13
101	2.54	3.06	3.22
102	2.04	2.08	2.98
103	2.84	2.95	3.47
104	3.75	3.72	4.15
105	3.53	3.24	4.28
106	3.11	2.68	3.14
107	3.43	3.11	3.3

It can be noted that the NSI follows the panel ratings more closely than the correlation between the PSI model, which is currently implemented by TxDOT, and the IRI. The two models differ the greatest on the upper and lower ends of the PSR ratings, i.e., the newer model rates the smoother roads rougher and the rougher roads smoother than does the current model. However, this is also the case when comparing the panel ratings to the current model.

3.2.2 NSI as Indicator of Localized Roughness [15]

The new equation relates user ride opinions to the physical wavelength characteristics of the associated pavement profile, unlike the current equation which is a related to IRI. Comparisons were made between the current and new ride equation for project 4901 and during a repeat verification of the NSI equation on profiles collected from test sections in Austin, it was noted that one section was significantly different from the previous measurements. In all earlier comparisons, as mentioned in the previous section, the new ride equation typically provided somewhat lower SI readings for smooth pavements and higher readings for the rough sections. These differences were for the most part never greater than 0.5 SI. Figure 3-4 illustrates the comparisons based on the 2001 data runs on the Austin Test Sections.

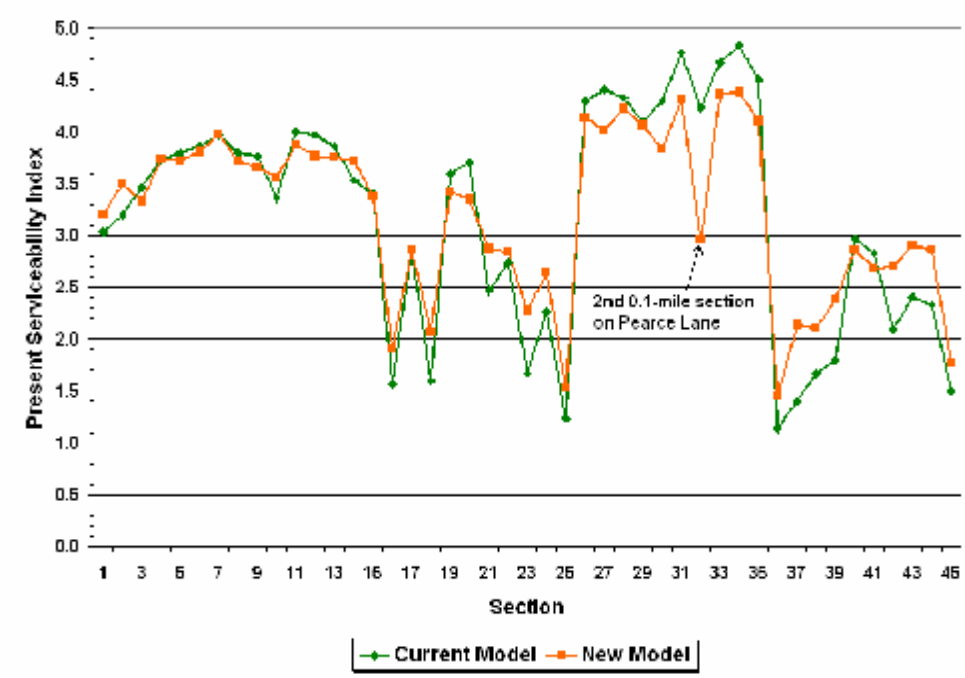

Figure 3-4 Comparisons between Current and New SI Models on Austin Sections [15]

As noted in the figure, the Sis computed between the current and new model on the second 0.1 mile section of Pearce Lane were significantly different (4.2 vs. 3.0) and had changed from a previous reading of 4.26 in less than three months. In further investigations, it was found that a pothole had formed in the left wheel path of this section (see Figure 3-6). The section was re-measured, this time driving to the right of the pothole, resulting in more consistent readings (current SI of 4.7 vs. new SI of 4.2).

Figure 3-5 Pot Hole in Wheel Path of the Second 0.1 mile Section along Pearce Lane

In further investigating the physical characteristics of the profile, it was noted that the wavelength of the pothole had a significant effect on the two of the wavelength amplitudes. This example further makes it appear that the new ride equation is a better indicator of sections with localized roughness than the current SI equation, and thus the IRI. The IRI statistic is based on the average of the predicted relative displacements between the sprung and unsprung masses of a quarter car model. Therefore, the effect of the pothole, although significant for short sections, is less over the 0.1 mile or 528 ft section. Also, the weights on the frequencies of IRI equation are fixed and are not selected based on the rating panel. Although the NSI model depends on the average amplitudes of the one to eight meter wavelengths, with eight statistics used to measure ride, it is more likely to better distinguish the pothole.

An example of this phenomenon was observed while validating the correlation between NSI and IRI.

3.2.3 NSI Computation

The real-time NSI program was run on an Intel i3 processor, that supports multithreading, which will be discussed in the next chapter. This program has been modified to support multithreading and to support real-time computation using the Real-time Embedded NSI

module. The multithreaded NSI application had two threads running on the processor: the first for acquisition of the profile data from the portable profiler discussed earlier, and the second thread called the processing thread for processing the received data from the profiler. The processing thread calculates NSI by following the steps shown below. Table 3-3 below compares the real time NSI readings to the post-processed NSI readings

1. The vector array frequency is set to the 8 frequencies
2. The rectangular window for the transformation is selected (only minor variations were observed between Rectangular, Hanning or Hamming windows). The power values are averaged over 64 points with non-overlapping intervals.
3. The thread checks the number of elements in the circular buffer storing the received profile data. If there is data equivalent to 52.8 ft in the buffer, this thread starts to compute the NSI using the left and right wheel path.
4. The difference between adjacent points are computed (derivative of x and y with respect to distance) to help offset non-stationary effects of the profile data. The average left and right profile values are obtained and placed in a temporary array.
5. The number of non-overlapping intervals (segments) is determined, the data are windowed.
6. The spectral components are computed in accordance with equation 3.2, and the average power values are computed and placed in an array, pds (power density spectrum).
7. The eight coefficients (α_1, α_2, α_3 … α_8) are placed in the array coef and the NSI is calculated by using equation 3.3.

Chapter 4

Portable NSI Module

The portable NSI module consists of a portable profiler, the real-time module, i.e. the Intel NUC kit, that processes the profile data, a network switch for switching the LAN connections between the portable profiler, real-time module and an external client PC used to display and record the profile and NSI data.

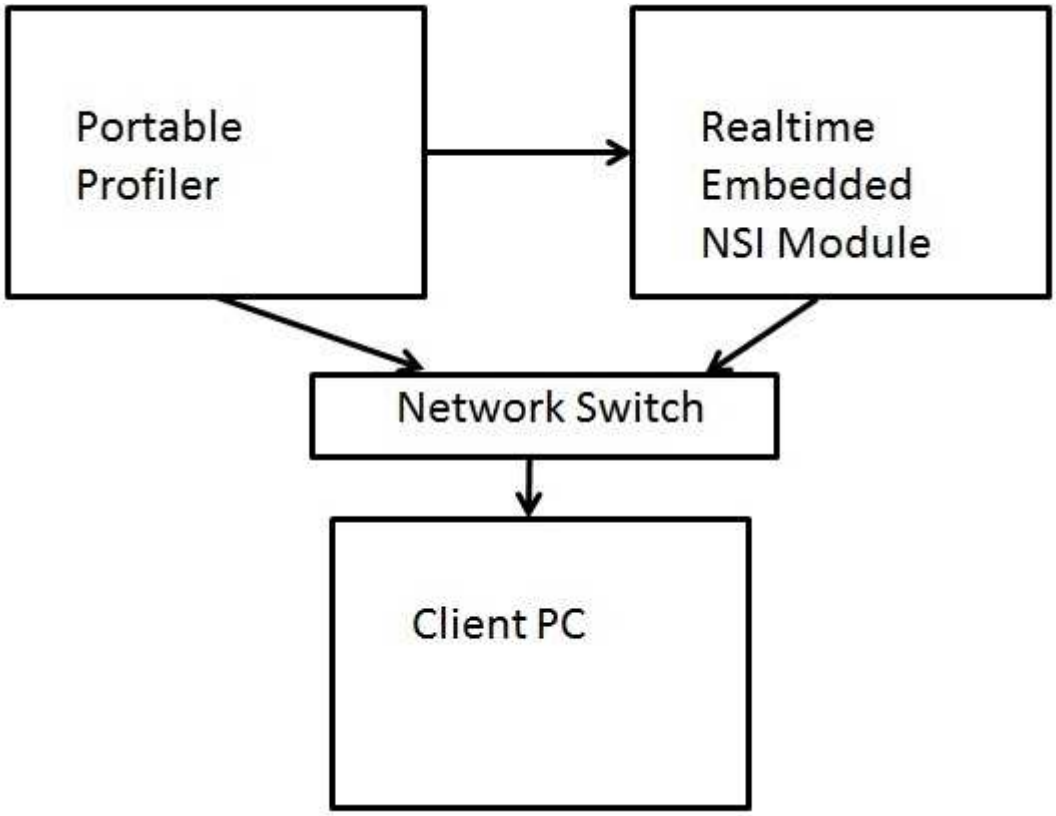

Figure 4-1 Portable NSI Module

4.1 Module Operation

4.1.1 Data Acquisition

The portable profiler collects the profile data as discussed in section 2.2 and sends the profile data in VNET protocol over the Ethernet to the network switch which is accessed by the client PC and the real-time embedded module. The client PC stores and displays the profile

data and the real-time module computes the NSI values over 0.01 mile sections and transmits the computed real-time NSI values over the Ethernet to the switch from where it is obtained by the client PC, which displays and stores the NSI data too.

The profiler continuously sends the profile data in VNet protocol. A multithreaded application running on the NUC acquires this data and writes it into a circular buffer using one thread, while the other thread polls the number of elements in the circular buffer. This thread waits until the data elements in the buffer measure up to a total of 52.8 ft. For example, if the profiler measures the wheel path every 0.960503 inch, there needs to be a total of 660 elements in the buffer with each element denoting the wheel path for each 0.960503 inch. When this number of elements or more is present in the circular buffer, the thread begins processing of this data to obtain the NSI by the steps mentioned in the previous chapter. The computed NSI values are sent to another client PC where it is displayed and stored.

4.1.2 Threads Running in the Module

The Windows threading API CreateThread( ), is used in the main thread to create two separate threads. One thread runs a TCP/IP server socket program to read the data at the socket and write it into a temporary buffer. This data is then parsed to obtain the left and right profile data points and the comments, if any. The parsed data is temporarily stored in a struct array from where it will be written to a circular buffer of the same struct type. The data structure was created to store all data associated with a single profile data point inside one variable. Before writing into the ring buffer, this thread checks the available space in the buffer and compares it to the number of elements stored in the temporary array. If the available space is less than the size in the array, the thread waits until the other thread clears some elements once they are processed. When sufficient space is available in the circular buffer, the data from the temporary array is pushed into the circular buffer and the write pointer is updated to point to the last free location in the buffer.

The second thread calculates the number of points required for processing NSI at an interval of 52.8ft and checks the circular buffer if it contains that many elements. If not, the thread waits until the server thread writes sufficient elements to the buffer. When the ring buffer has the required number of elements, these elements are moved into another temporary array and the circular buffer is freed of those elements. Now, we have a section ready to be processed.

4.1.3 Calculating NSI with Parallel Processing

The section data available for processing, discussed above, is then filtered of high frequencies to avoid noise components. Linear trends are removed from the left and right profile data to ensure that the power spectrum of this data is a Gaussian distribution. The left and right profile data are averaged together into a single array of profile data.

To calculate the power spectral components of the 8 frequencies, as required by equation 3.3, the DFT for each of the frequencies is determined. The real and imaginary parts of each frequency component is calculated and multiplied. The *spcomp* function computes a single complex DFT component for a given frequency. Parallel processing is implemented in computing the real and imaginary parts of the DFT components and its vector multiplication with the help of OpenMP. The compiler directive *#pragma omp parallel for* tells the compiler that the *for* loop which immediately follows can be executed in parallel. It may do it in an arbitrary order and each thread gets a different section of the loop and these sections are executed in parallel. The application of *#pragma omp parallel* to parallelize the power spectral computation in the NSI program is shown below.

```
#pragma omp parallel for
for(iIndex=0;iIndex<8;iIndex++)
{
    delta_freq[iIndex] = freq[iIndex]*dDistanceInterval;
    tempcpx=spcomp(g_dDataVector,&NDFT,&delta_freq[iIndex]);
```

```
        g_ComplexVector[iIndex].i=tempcpx.i;
        g_ComplexVector[iIndex].r=tempcpx.r;
    }
    #pragma omp parallel for
    for(iIndex=0;iIndex<8;iIndex++)
    {
        result = multComplex(g_ComplexVector[iIndex],(tsv*nsgmts));
        pds[iIndex] = pds[iIndex]+result;
    }
```

4.2 Intel NUC

Next Unit of Computing (NUC) is a small form factor PC designed by Intel, used to implement the real-time module. The second generation NUC, used for this project, is based on the Ivy Bridge Core i3 processor. The second generation DC3217BY NUC kit was used in this project for processing applications. The NUC kit consists of the board in a plastic case with a fan and an external power supply. The board contains a non-removable ultra low voltage 1.8GHz Core i3-3127U processor and QS77 Express chipset. Optional components include an mSATA solid state drive and a Wi-Fi/Bluetooth radio.

The NUC can be connected to the portable profiler to acquire the real-time profile data either via Wi-Fi or through physical LAN connection.

4.2.1 Intel i3 processor

The mobile 3rd Generation Intel Core i3 processors are the next generation of 64-bit, multi-core mobile processors built on 22-nanometer processor technology. The processor is designed for a two-chip platform. The two-chip platform consists of a processor and a Platform Controller Hub (PCH) and enables higher performance, lower cost, easier validation and improved x-y footprint. The processor includes Integrated Display Engine, Processor Graphics

and an Integrated Memory Controller. This processor is designed for mobile platforms like the NUC described in the previous section.

The processor supports Intel Hyper-Threading Technology that allows an execution core to function as two logical processors. While some execution resources such as caches, execution units and buses are shared, each logical processor has its own architectural state with its own set of general-purpose registers and control registers. This feature along with the two processor cores facilitates the multithreaded application running on the NUC.

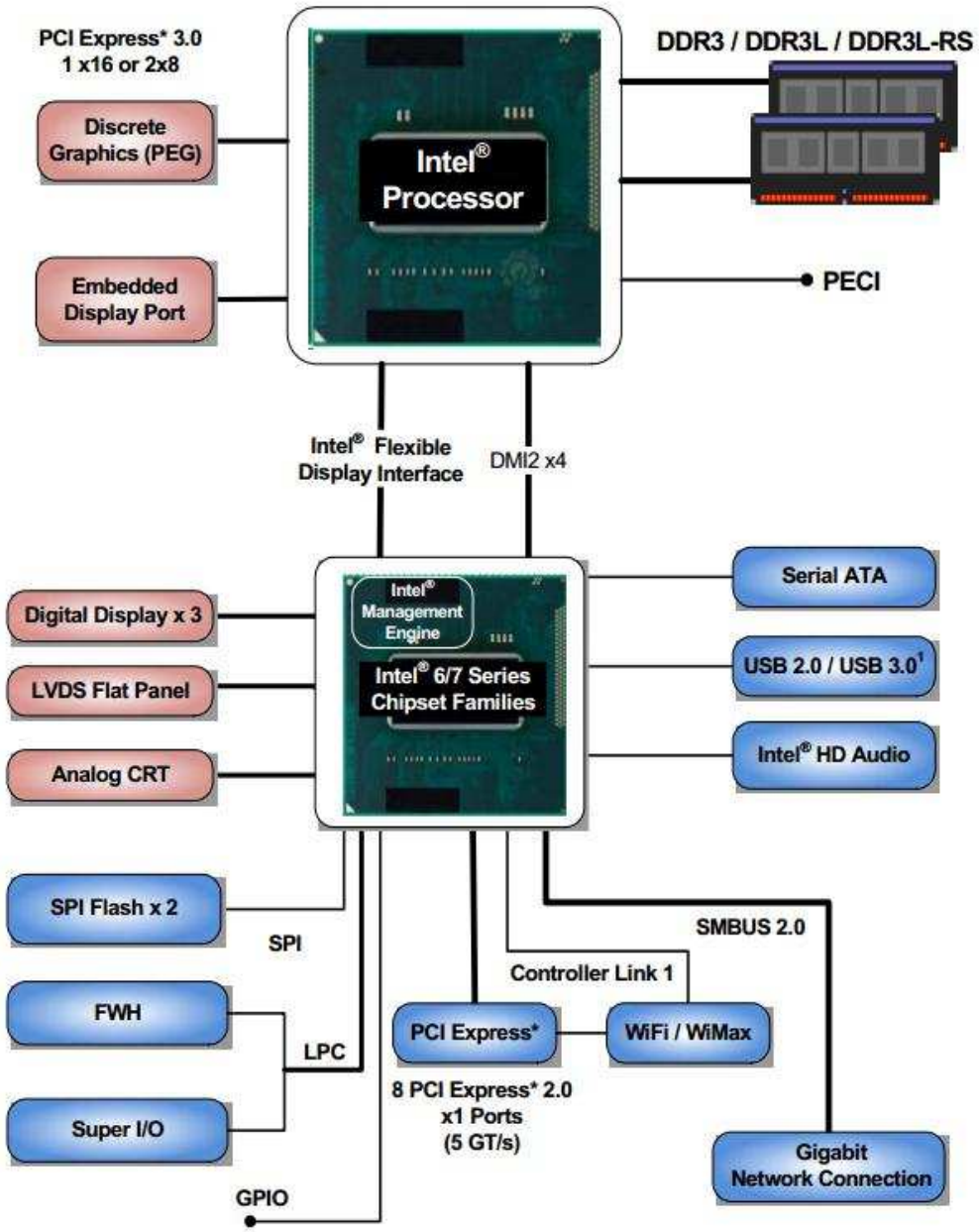

Figure 4-2 Intel mobile processor platform

Chapter 5

Comparisons and Results

5.1 Real-time vs post-processed NSI

Table 5-1 Comparison between Real-Time and Post Processed NSI Readings

Distance	Real-time NSI	Post-processed NSI
0.00	3.75	3.75
0.01	3.18	3.18
0.02	4.33	4.33
0.03	3.97	3.97
0.04	4.08	4.08
0.05	3.38	3.38
0.06	3.54	3.54
0.07	3.75	3.75
0.08	3.77	3.77
0.09	4.20	4.20
0.10	3.92	3.92
0.11	3.99	3.99
0.12	4.13	4.13
0.13	4.00	4.00
0.14	3.49	3.49
0.15	3.60	3.60
0.16	3.73	3.73
0.17	3.62	3.62
0.18	3.48	3.48
0.19	4.43	4.43
0.20	4.41	4.41
0.21	4.07	4.07
0.22	2.80	2.80
0.23	3.50	3.50
0.24	4.62	4.62
0.25	3.55	3.55
0.26	4.11	4.11
0.27	3.32	3.32
0.28	3.21	3.21

Table 5-1 continued

0.29	4.04	4.04
0.30	3.89	3.89
0.31	3.25	3.25
0.32	3.75	3.75
0.33	3.08	3.08
0.34	3.11	3.11
0.35	3.64	3.64
0.36	3.09	3.09
0.37	3.62	3.62
0.38	3.10	3.10
0.39	4.30	4.30
0.40	4.59	4.59
0.41	4.14	4.14
0.42	3.11	3.11
0.43	4.03	4.03
0.44	3.56	3.56
0.45	3.51	3.51
0.46	3.72	3.72
0.47	3.36	3.36
0.48	3.69	3.69
0.49	3.59	3.59
0.50	2.53	2.53
0.51	4.58	4.58
0.52	4.23	4.23
0.53	3.80	3.80
0.54	4.67	
0.55	4.44	
0.56	3.39	
0.57	3.87	
0.58	5.00	
0.59	3.97	
0.60	3.78	
0.61	2.28	
0.62	4.12	

Table 5-1 continued

0.63	3.57	
0.64	3.50	
0.65	3.84	
0.66	3.40	
0.67	3.34	
0.68	3.93	
0.69	4.69	
0.70	4.49	
0.71	3.06	
0.72	3.75	
0.73	3.87	
0.74	3.73	
0.75	4.38	
0.76	3.51	
0.77	3.66	
0.78	4.65	
0.79	3.86	
0.80	3.62	
0.81	3.99	
0.82	3.36	
0.83	4.14	
0.84	3.41	
0.85	4.46	
0.86	4.26	
0.87	3.33	
0.88	3.64	
0.89	3.85	
0.90	4.52	
0.91	3.88	
0.92	4.01	
0.93	3.41	
0.94	4.11	
0.95	4.15	
0.96	4.17	

Table 5-1 continued

0.97	3.53	
0.98	4.03	
0.99	3.55	
1.00	3.70	
1.01	4.27	
1.02	3.90	
1.03	4.58	
1.04	3.91	
1.05	4.39	
1.06	4.16	
1.07	4.28	
1.08	4.10	
1.09	3.73	
1.10	4.15	
1.11	3.35	
1.12	4.54	
1.13	4.01	
1.14	3.77	
1.15	3.18	
1.16	4.32	
1.17	4.26	
1.18	4.50	
1.19	3.41	
1.20	3.52	
1.21	3.79	
1.22	4.04	
1.23	4.01	
1.24	4.35	
1.25	3.95	
1.26	4.24	
1.27	3.61	
1.28	3.53	
1.29	3.88	
1.30	3.80	

Table 5-1 continued

1.31	3.58	
1.32	3.19	
1.33	4.33	
1.34	4.05	
1.35	4.07	
1.36	2.37	
1.37	3.42	
1.38	4.12	
1.39	3.43	
1.40	4.42	
1.41	3.39	
1.42	3.27	
1.43	3.56	
1.44	4.07	
1.45	3.14	
1.46	3.71	
1.47	3.00	
1.48	2.96	
1.49	3.83	
1.50	2.97	
1.51	3.65	
1.52	3.20	
1.53	4.06	
1.54	4.51	
1.55	3.49	
1.56	3.34	
1.57	3.86	
1.58	3.78	
1.59	3.50	
1.60	3.62	
1.61	3.46	
1.62	3.65	
1.63	3.03	
1.64	3.34	

Table 5-1 continued

1.65	4.59	
1.66	4.50	
1.67	3.63	
1.68	4.32	
1.69	4.38	
1.70	3.34	
1.71	3.77	
1.72	3.94	
1.73	3.98	
1.74	3.72	
1.75	3.18	
1.76	4.20	
1.77	3.99	
1.78	3.39	
1.79	5.00	
1.80	3.58	
1.81	3.23	
1.82	3.80	
1.83	4.71	
1.84	4.56	
1.85	2.88	
1.86	3.74	
1.87	3.97	
1.88	3.51	
1.89	4.42	
1.90	3.48	
1.91	3.82	
1.92	4.45	
1.93	3.71	
1.94	3.74	
1.95	4.11	
1.96	3.07	
1.97	4.01	
1.98	3.47	

Table 5-1 continued

1.99	4.13	
2.00	3.88	
2.01	3.47	
2.02	3.71	
2.03	4.25	
2.04	4.52	
2.05	3.69	
2.06	4.29	
2.07	3.26	
2.08	4.14	
2.09	3.86	
2.10	4.21	
2.11	3.36	
2.12	4.01	
2.13	3.43	
2.14	4.18	
2.15	4.13	
2.16	4.02	
2.17	4.52	
2.18	3.79	
2.19	4.23	
2.20	4.00	
2.21	4.33	
2.22	4.29	
2.23	3.70	
2.24	3.91	
2.25	3.33	
2.26	3.27	
2.27	4.06	
2.28	3.91	
2.29	2.71	
2.30	4.14	
2.31	4.37	
2.32	4.65	

Table 5-1 continued

2.33	3.65	
2.34	3.75	
2.35	3.88	
2.36	4.52	
2.37	3.86	
2.38	4.58	
2.39	4.01	
2.40	5.00	
2.41	3.71	
2.42	3.64	
2.43	3.98	
2.44	3.76	
2.45	3.47	
2.46	2.57	
2.47	4.07	
2.48	4.00	
2.49	4.22	
2.50	2.49	
2.51	3.33	
2.52	3.72	
2.53	3.44	
2.54	4.65	
2.55	3.43	
2.56	3.07	
2.57	3.33	
2.58	4.21	
2.59	3.14	
2.60	3.67	
2.61	2.85	
2.62	3.14	
2.63	4.11	
2.64	3.07	
2.65	3.84	
2.66	3.18	

Table 5-1 continued

2.67	3.81	
2.68	4.47	
2.69	3.47	
2.70	3.61	
2.71	3.48	
2.72	4.02	
2.73	3.55	
2.74	3.68	
2.75	3.70	
2.76	3.68	
2.77	3.28	
2.78	3.63	
2.79	4.65	
2.80	4.32	
2.81	3.54	
2.82	3.85	
2.83	4.32	
2.84	3.31	
2.85	3.78	
2.86	3.50	
2.87	4.16	
2.88	3.65	
2.89	3.67	
2.90	4.32	
2.91	4.05	
2.92	3.35	
2.93	4.92	
2.94	3.77	
2.95	3.32	
2.96	3.50	
2.97	4.63	
2.98	4.66	
2.99	2.77	

Note that the profile data up to 0.53 miles was available, which was looped again and again by the profiler simulation to generate profile data up to 3 miles and more. The real-time NSI output confirms with the post-processed NSI output for this length of data and gives a consistent output that relates to the looped profile data.

5.2 NSI vs IRI comparison

A comparison between NSI and IRI was performed by calculating the NSI for 4 different road profiles collected and correlating those to the corresponding IRI values of the profile. The plots for these individual profiles are shown in Figure 5-1 through Figure 5-4 and an average of all these is plotted in Figure 5-5. It was found that overall, the NSI correlated to the IRI with R^2 = 0.863.

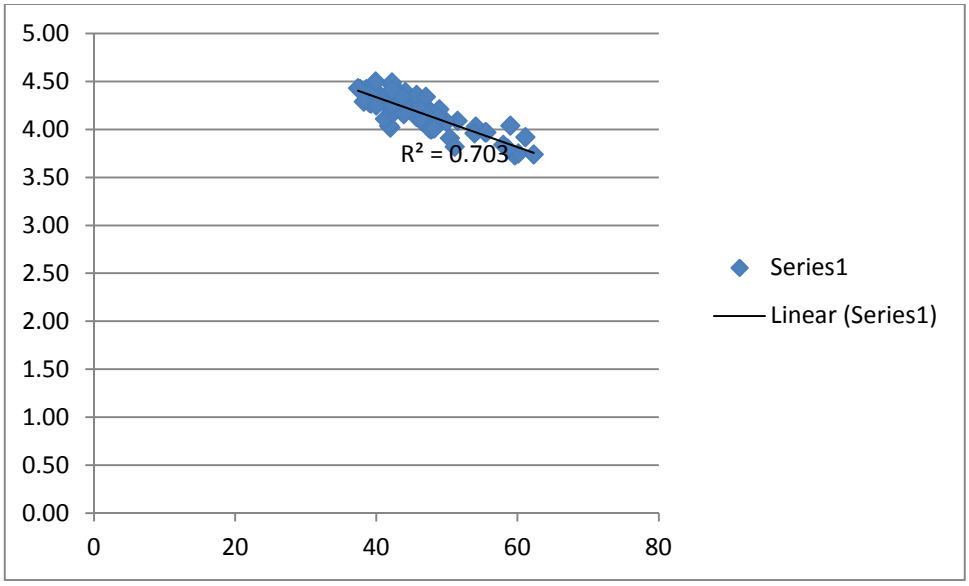

Figure 5-1 IRI vs NSI plot for section 1

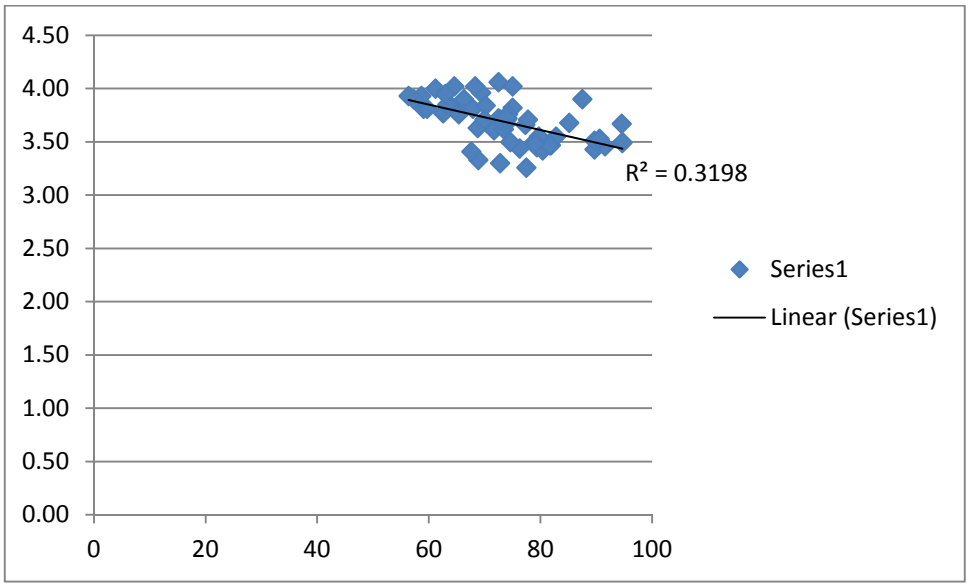

Figure 5-2 IRI vs NSI plot for section 2

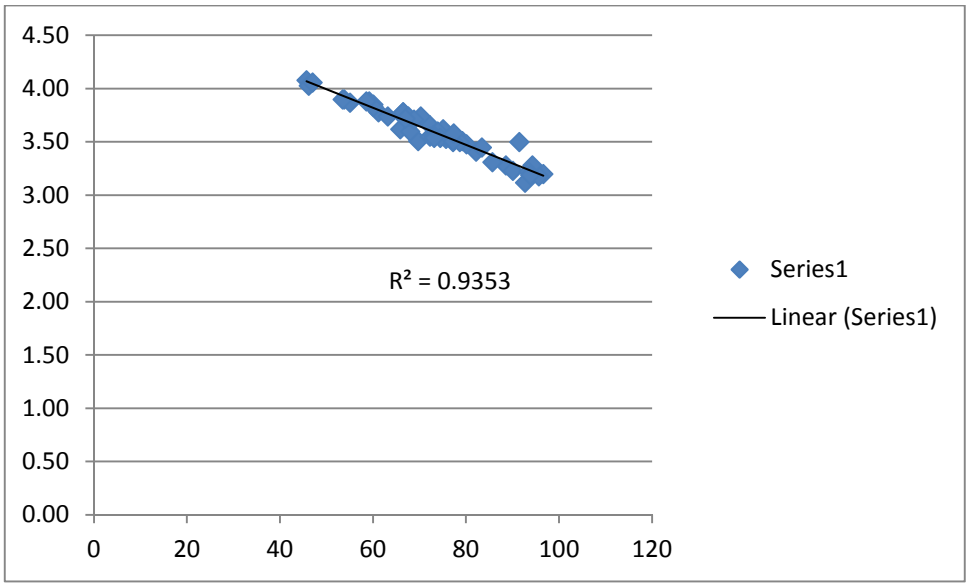

Figure 5-3 IRI vs NSI plot for section 3

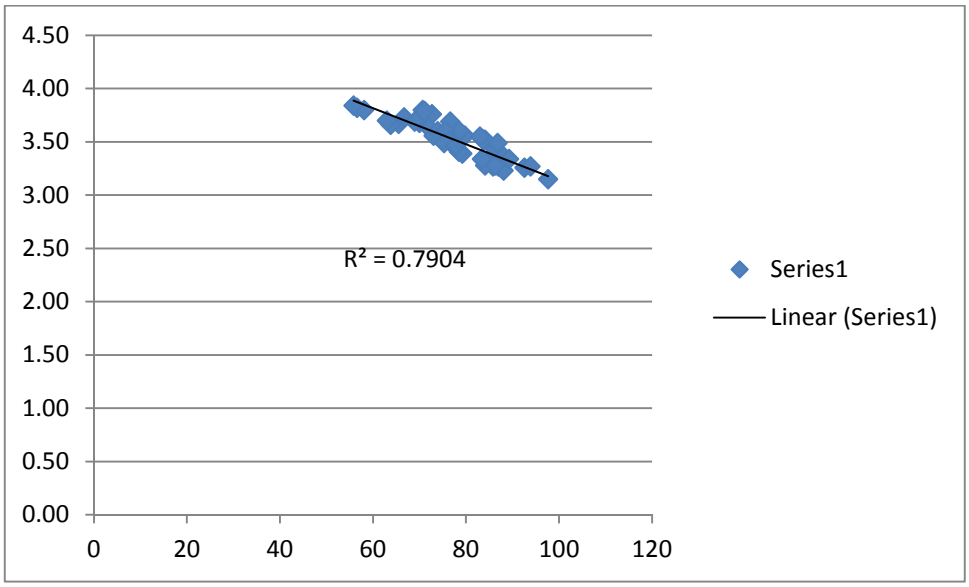

Figure 5-4 IRI vs NSI plot for section 4

It can be noted that Figure 5-2 is least correlated compared to the other three plots. There are a couple of points that have low NSI compared to a high NSI value. For 3 consecutive runs over this 0.1 mile section, the IRI values were calculated to be 68.9, 72.8 and 67.6, and the corresponding NSI values were calculated as 3.33, 3.30 and 3.41 respectively. Therefore, the IRI marks this section as an average section whereas the NSI consistently marks it as a rough section.

There are also some points that show higher NSI values than expected for a particular IRI value. This couldn't be completely understood.

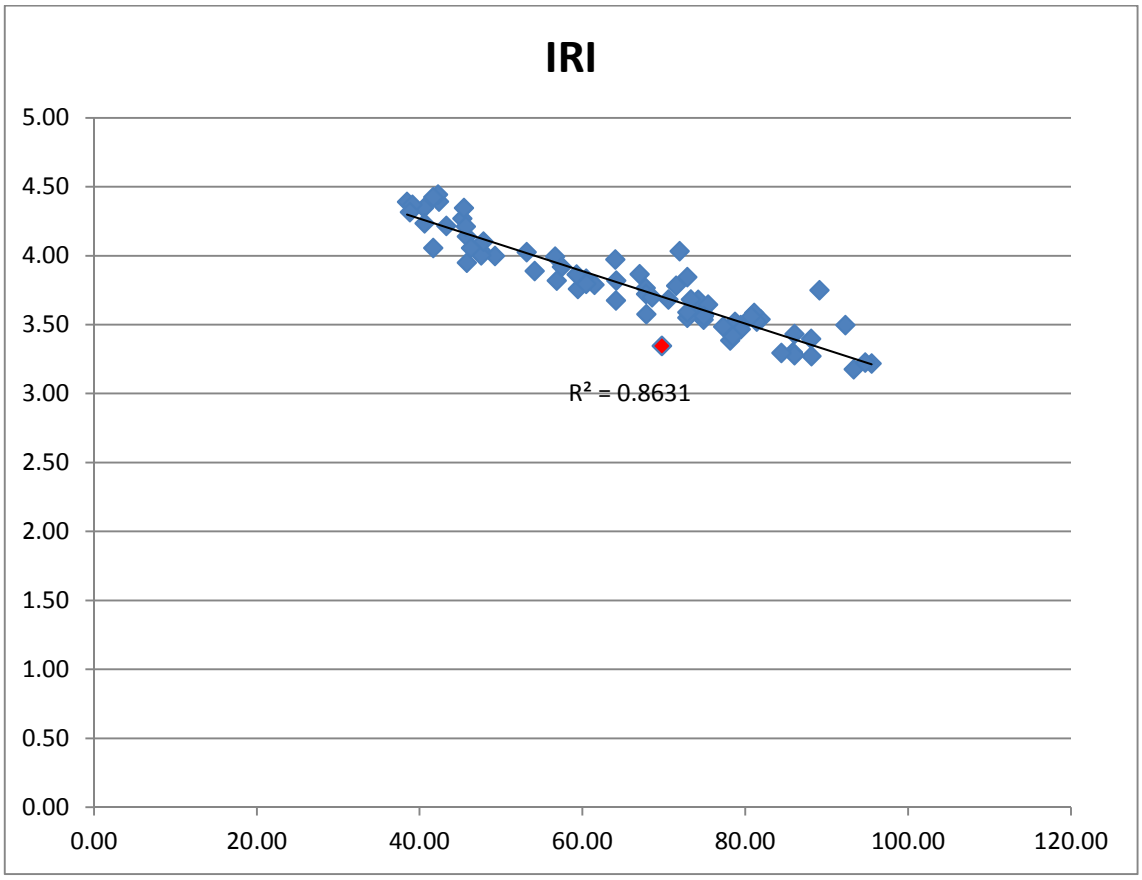

Figure 5-5 Overall IRI vs NSI plot

Note the data point marked in red in the above plot. It corresponds to a mismatch between the IRI and the NSI in one of the sections of the pavements studied. The point corresponds to an IRI value of 69.77, which denotes an average level of smoothness, as opposed to the NSI value 3.35, which stands for a rough section. A continuous IRI over 52.8ft sections is plotted in Figure 5-6.

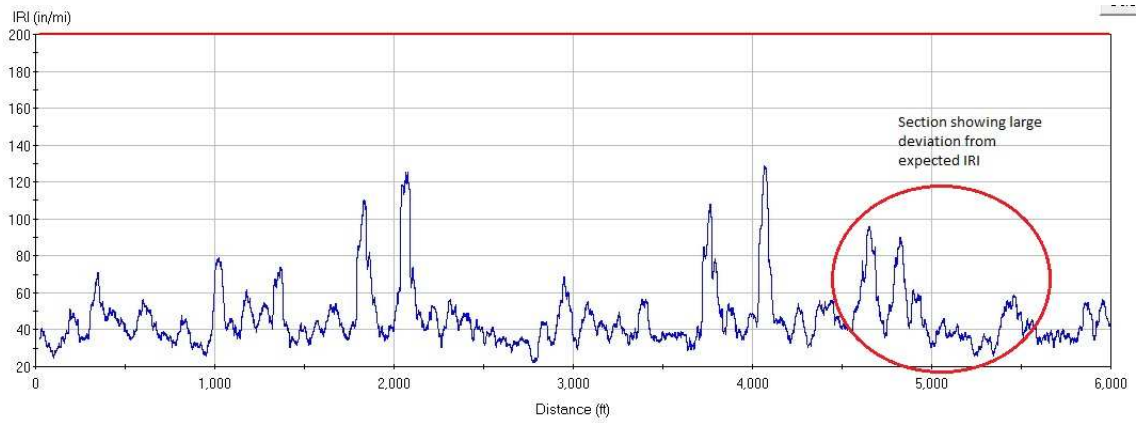

Figure 5-6 Continuous IRI plot

The portion circled in red is an approximate of the section exhibiting a variance from the expected NSI range. It can be noted that there is some rough patches in the section that raise the IRI of those parts as high as upper 90s, which is an indication of roughness. These patches are followed by some smooth road with the IRI falling as low as 30, which denotes a very smooth portion. Thus, they average out over 0.1 miles to give an IRI value corresponding to a section of average smoothness when there are rough regions within the section. This is similar to the pothole incident along Pearce lane, discussed earlier in section 3.2.2 and illustrated in Figure 3-5.

Chapter 6

Conclusions and Future Work

This thesis presented an investigation of a pavement surface defect measurement system as a way to measure the ride quality of the road continuously over a long stretch of road. Simulation was performed for the checking the feasibility of conducting surveys for long sections. The results of this simulation provided insights into this method. Simulations were also adjusted to mock the variation in speed of the profiling vehicle. It was noted that the processing was done irrespective of the speed of the vehicle.

The explored method could add an additional functionality in the future to perform stop-go profiling and computation. This method could also be directly integrated into the portable profiler that was developed in the Transportation Instrumentation Laboratory at UTA.

References

1. M.W. Sayers, S.M. Karamihas and University of Michigan, *The little book of profiling: basic information about measuring and interpreting road profiles,* Transportation Research Institute, 1998.
2. Carey, W.N., Irick, P.E.; *The Present Serviceability Performance Concept*; Highway Research Board, Bulletin 250, National Research Council; Washington, DC; 1960.
3. Al-Omari, B., Darter, M.I.; *Relationships between International Roughness Index and Present Serviceability Rating*; Transportation Research Record No. 1435 Pavement and Traffic Monitoring and Evaluation; National Academy Press; Washington; DC;. 1994.
4. LeClerc, R. V., Marshall, T. R. “Washington Pavement Rating System - Procedures and Application”, presentation at the Western Summer Meeting of the Highway Research Board Sacramento, California, August 1970.
5. Shahin, M.Y., Darter, M.I., Kohn, S.D.; *Development of a Pavement Maintenance Management System, Vol I, II, V, Airfield Pavement Condition Rating*; US Air Force Civil Engineering Center; 1976.
6. Nair, S. K., W. R. Hudson, and C. E. Lee. *Realistic Pavement Serviceability Equations Using the 690D Surface Dynamics Profilometer.* Research Report 354-1F, Center for Transportation Research, The University of Texas at Austin, Austin, Texas, 1985.
7. Deighton, R., Sztraka, J., *Pavement Condition*, dTV Technical Guide (Volume 3), published by Deighton Associates Limited, 1995.

8. Roberts, F. L., and W. R. Hudson. *Pavement Serviceability Equations Using the Surface Dynamics Profilometer*. Research Report 73-3, Center for Highway Research, The University of Texas at Austin, Austin, Texas, 1970.
9. Stearns, Samuel D., David, Ruth A., *Signal Processing Algorithms in MATLAB*, Prentice Hall, Upper Saddle River, NJ, 1996.
10. Walker, R.S. and W. Ronald Hudson, *The Use of Spectral Estimates for Pavement Characterization*, Research Report 156-2, Center for Highway Research, The University of Texas at Austin, August 1973.
11. Walker, Roger S., and W. R. Hudson, *A Correlation Study of the Mays Road Meter with the Surface Dynamics Profilometer,* Research Report 156-1, Center for Highway Research, The University of Texas at Austin, February 1973.
12. Walker, Roger S., Freddy L. Roberts, and W. R. Hudson*, A Profile Measuring, Recording, and Processing System*, Research Report 73-2, Center for Highway Research, The University of Texas at Austin
13. Walker, Roger S. and Fernando, Emmanuel, *Evaluation of Ride Equation using Current Profiler Systems and New Sensor Technology*, Research Report 4901F, Transportation Instrumentation Laboratory, The University of Texas at Arlington, The Texas Transportation Institute, Texas A&M University, 2002
14. Akhter, Shameem and Roberts, Jason, *Multi-Core Programming – Increasing Performance through Software Multi-threading*, Intel Press, 2006
15. Walker, Roger S. and Fernando, Emmanuel A. Portable Profiler for Pavement Profile Measurements – Final Report, Research Report 0-6004-2,, Transportation Instrumentation Laboratory, The University of Texas at Arlington, The Texas Transportation Institute, Texas A&M University, 2002

Biographical Information

Vivek Jolly was born in Kerala, India in 1988. He received the Bachelor of Technology in Applied Electronics and Instrumentation Engineering from Mahatma Gandhi University in 2010. He enrolled in the Master of Science in Electrical Engineering program at The University of Texas at Arlington (UTA) in 2012. While studying at UTA, he did various projects in the field of microprocessor and microcontroller embedded systems, signal processing and wireless communication. He started his research at the Transportation and Instrumentation Laboratory in the CSE department of UTA. His research interests include embedded microcontroller systems, signal processing and road profiling.